Temperature Studies of the Scintillating Tileboards for CMS HGCAL Upgrade

Marius Wilm Menzel, University of Heidelberg

September 9, 2021

Abstract

The High Luminosity upgrade of the LHC (HL-LHC) will increase the luminosity of the experiment by several magnitudes which results in a high pile-up within the detectors. As a result, the CMS experiment's end-cap calorimeters will be replaced with a highly granular calorimeter (HGCAL). For the upgrade of the hadronic part, new scintillating tileboards using Silicon Photo Multipliers (SiPMs) are developed. In the final experiment, the tileboards will be operated at $-30°C$. In this report, the functionality of the tileboard was verified down to $-40°C$ and the gradient of the overvoltage with temperature was found to be $(33 \pm 2)\frac{mV}{°C}$ for $2mm^2$ SiPMs and $(31 \pm 1)\frac{mV}{°C}$ for $4mm^2$ SiPMs. Furthermore, the noise dependence on temperature for irradiated SiPMs was investigated.

1 Introduction

The Compact Muon Solenoid (CMS) is one of the four major experiments carried out at the Large Hadron Collider (LHC) at CERN, Switzerland. CMS is a multi-purpose high-energy physics experiment and was part of the discovery of the Higgs boson in 2012.

1.1 CMS High Granularity Calorimeter

The High Luminosity Large Hadron Collider (HL-LHC) project is dedicated to increase the number of collisions by a factor of five to seven by the year 2027. In order to ensure that the CMS detector is capable of the increasing rates, several subsystems of the detectors have to be upgraded. The CMS Hadronic Calorimeter (HCAL) is upgraded to the High Granularity Calorimeter (HGCAL), which provides improved energy as well as increased spatial resolution in order to prevent pile-up. The HGCAL endcap, which is depicted in Figure 1, consists of two major parts: the electromagnetic calorimeter (CE-E), which consists of hexagonal silicon sensor modules, and the hadronic calorimeter (CE-H), which is based on silicon sensor modules and trapezodial scintillator tileboards. This report will focus on tests with the scintillating tileboards.

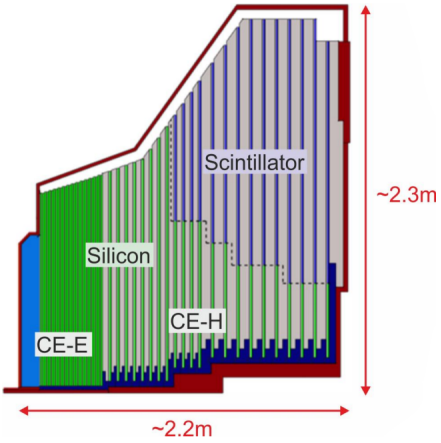

Figure 1: Sketch of the cross-section of the HGCAL endcap. Taken from [1].

1.2 Scintillating Tileboards

The scintillator tileboards for the HGCAL upgrade come in 8 major geometries with areas ranging from $21 \times 15\ cm^2$ to $45 \times 42\ cm^2$. The board investigated in this report consists of 64 channels, from which 16 are equipped. Here, one channel consists of a scintillating tile, which is wrapped in reflecting silver foil and glued on top of a Silicon Photo Multiplier (SiPM). When a charged particle passes through the scintillating tile, it excites atoms in the crystal. By the following de-excitation, photons will be emitted, whose number is proportional to the energy of the traversing particle. The photons will

then be reflected by the foil and a fraction of it can be detected by the SiPM. A cross section of this can be seen in Figure 2a.

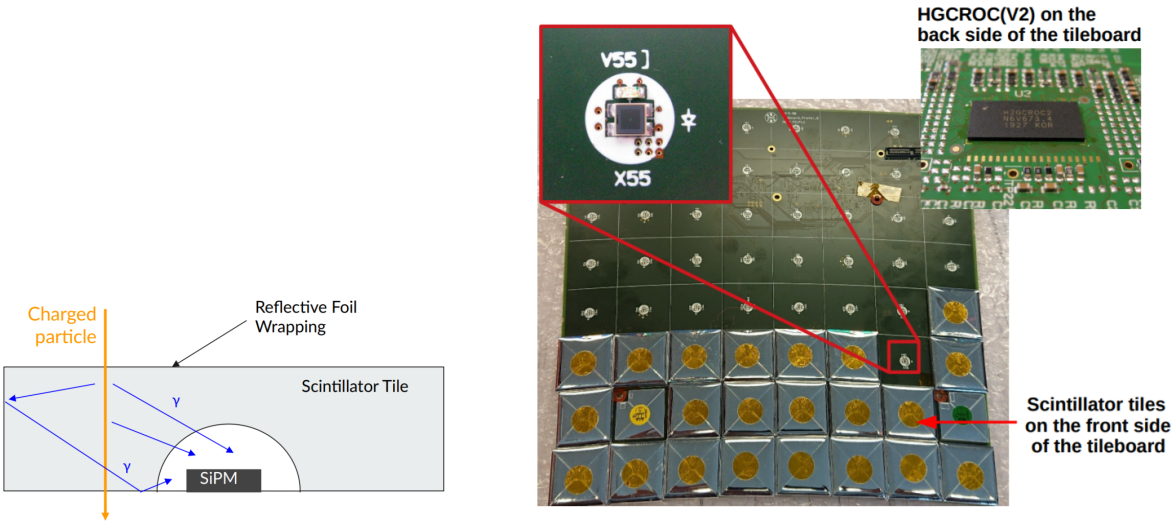

(a) Cross section of a scintillating tile glued on a SiPM

(b) Prototype of the tileboard.

Figure 2: Functionality and composition of the scintillating tileboard. Taken from [2].

With a very low-intensity LED placed next to the SiPM, the tileboard provides the opportunity to test the channels functionality as well as to calibrate it without using external sources. The information of all channels is read out and pre-processed by the Highly Granular Calorimeter Read Out Chip (HGCROC). From there, the signals are forwarded to the Data Acquisition. A photograph of the investigated tileboard with the SiPMs and the HGCROC can be seen in Figure 2b.

1.3 SiPMs

SiPMs are single-photon-sensitive detectors based on silicon. They consist of a matrix of Single Photon Avalanche Photo Diodes (SPADs) connected in parallel. SPADs consist of two major zones: the absorption region and the multiplication region. Here, the absorption region consists of pn-junctions as shown in Figure 3a. Due to the effects of the pn-junctions, a multiplication region is formed within the semiconductor. Electrons within this region are accelerated by the electric field which causes atoms within the semiconductor to ionize creating more electron-hole pairs. These secondary electrons also get accelerated within the electric field causing more and more atoms to ionize creating an avalanche resulting in a measurable signal. Here, the strength of the electric field within the multiplication region is given by the overvoltage (OV), e.g. the difference between bias and breakdown voltage:

$$OV = V_{bias} - V_{breakdown} \tag{1}$$

1.4 Gain Measurement using Single Photon Spectra

If one fills a histogram with the time-integration of the SiPM pulses and the SNR is sufficiently high, a spectrum as in Figure 3b is obtained. This is referred to as a Single Photon Spectrum (SPS). Depending on the light intensity, the spectrum can contain a different number of peaks. Here, the peak with the lowest ADC value corresponds to the pedestal voltage level of the SiPM. With increasing ADC value, the peaks can be assigned to the number of photons detected within one measurement time frame (25 ns). Here, the difference between the peaks directly corresponds to the SiPM´s gain. In order to quantify it, the spectrum is fitted using ROOT's TSpectrum class and the gain is extracted from the corresponding fit parameter. Additionally, the Noise can be characterized by the RMS of the pedestal value.

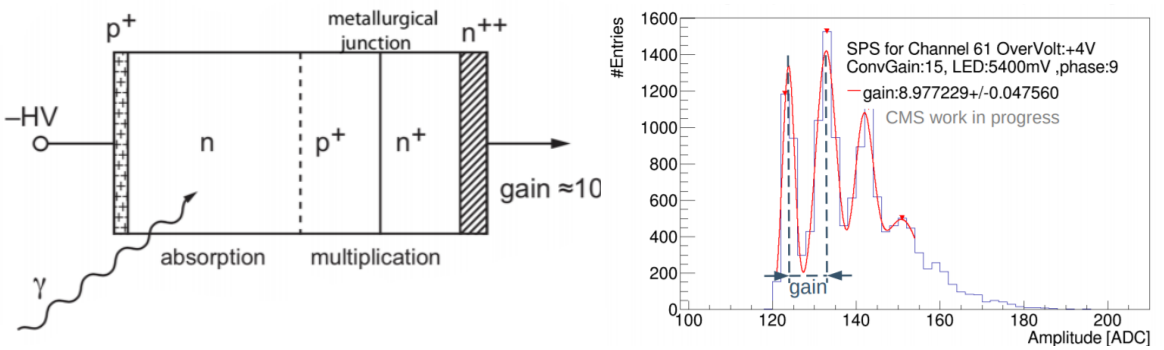

(a) Sketch of an SPAD. Taken from [3].

(b) Example of a recorded SPS. Taken from [2].

Figure 3: Photon detection with SiPMs

1.5 DNL correction

Differential Non-Linearity (DNL) is an effect generally occuring within Analogue to Digital Converters (ADCs). Within the HGCROC, every odd ADC tick of the output value varies in size. As a result, every second bin of the SPS receives systematically more hits than the bins in between. Due to this, the peaks of the SPS turn out to be non-gaussian, as one can see in Figure 4a. In order to correct for this effect, the same SPS is measured at three different pedestal values thereby distributing the DNL effects to different ADC bins. By shifting the three measured spectra on top of each other and adding up their entries, the corrected SPS is obtained. This method was first used to correct the DNL within the scope of this report. An example of a corrected spectrum is shown in Figure 4b. From here, it is clearly visible that all peaks of the SPS now show a Gaussian behaviour.

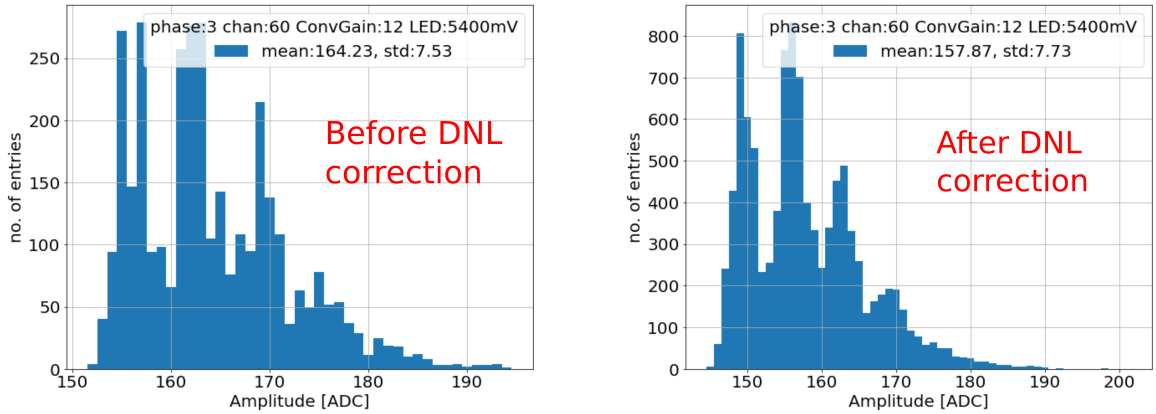

(a) SPS before DNL correction (b) SPS after DNL correction

Figure 4: Effect of the DNL correction on the SPS shape

2 Temperature Studies

Within the CMS detector, the tileboards will be operated at a temperature of $-30\,°C$ in order to reduce the electronical noise of the detector. Therefore, the functionality and the behaviour of noise and overvoltage regarding low temperatures has to be investigated.

2.1 Setup

For the measurements at different temperatures, the tileboard is placed in a climate chamber as shown in Figure 5b. The necessary operation voltages are provided via an adapter connected to a power supply. The signals from the tileboard channels are directed an pre-processed by a FPGA into binary files used for the further analysis.

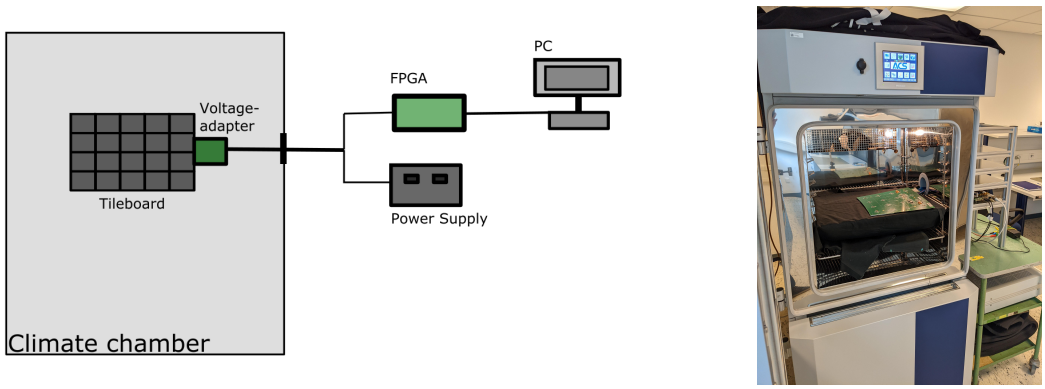

(a) Schematic of the temperature setup (b) Photo of the tileboard inside the climate chamber

Figure 5: Temperature Setup

2.2 Overvoltage Measurements

Since the OV describes the strength of the electric field in the multiplication region and therefore directly affects the amount of charge released in the electron avalanche, the gain is proportional to the OV. In order to quantify this effect, the SPS at three different OVs of 3 V, 4 V and 6 V was measured. Here, the SPS were taken at LED voltages from 5200 mV to 5400 mV in steps of 100 mV. The gain was then averaged over the light intensities. Additionally, the signal was sampled at the maximum amplitude to ensure maximum gain. Furthermore, the data was corrected for differences of breakdown voltages between the used SiPM-channels. The data together with a linear fit for each channel is shown in Figure 6.

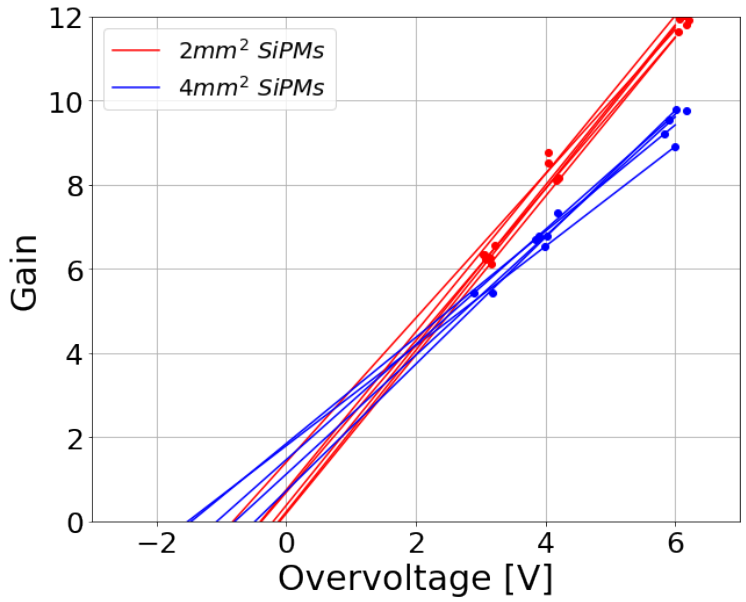

Figure 6: Measured OV dependence on the Gain at room temperature

Here, it can be seen that the gains for the $2mm^2$ SiPMs are systematically higher than for the $4mm^2$ SiPMs. Since both dependencies are expected to converge at zero, this results in different slopes for the two SiPM types. A possible reason for the systematic difference is the fact that the $4mm^2$ SiPMs consist of a larger number of SPADs resulting into a higher effective capacitance than for the $2mm^2$ SiPMs. This difference directly affects the pulse shapes from the SiPMs as illustrated in Figure 7. From the fit, the gradients ($\frac{\Delta Gain}{\Delta OV}$) for the respective SiPM type is determined to be:

$$\left(\frac{\Delta Gain}{\Delta OV}\right)_{2mm^2} \approx (1.85 \pm 0.07)/V \tag{2}$$

$$\left(\frac{\Delta Gain}{\Delta OV}\right)_{4mm^2} \approx (1.31 \pm 0.13)/V \tag{3}$$

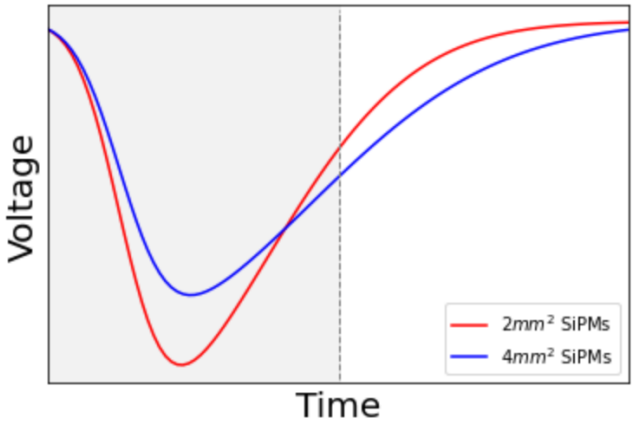

Figure 7: Illustration on the SiPM area influence on the measured gain

2.3 Temperature Measurements

Since the breakdown voltage increases with higher temperatures, the overvoltage lowers according to Equation 1. This also directly reduces the SiPM's gain. In order to quantify the gain behaviour with lower temperatures, the gain measurement as explained in Section 1.4 was carried out from room temperature (23 °C) down to −10 °C. The result is illustrated in Figure 8.

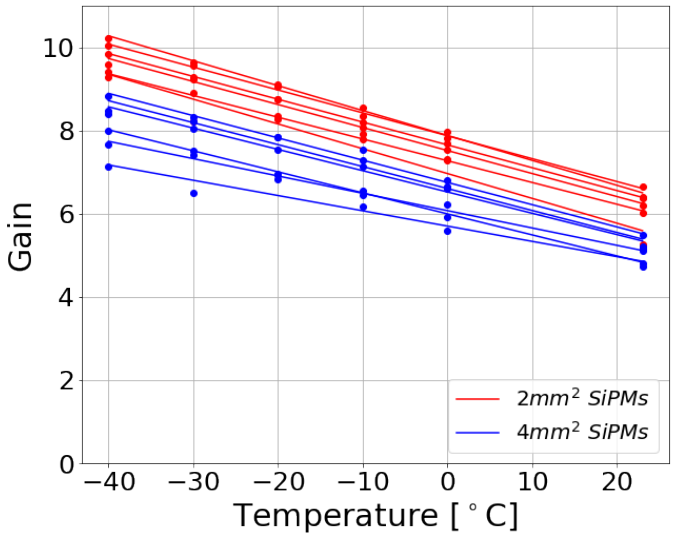

Figure 8: Measued temperture denpendence of the gain

Here, one can see that the gain behaves linear for all measured channels. Equivalent to Section 2.2, the $2mm^2$ SiPMs show a systematically higher gain than the $4mm^2$ SiPMs. From the fits the average slope of the two SiPM types was found to be:

$$\left(\frac{\Delta Gain}{\Delta T}\right) \approx -0.05/^{\circ}C \tag{4}$$

2.4 Overvoltage Temperature Dependence

In order to determine the temperature dependence of the OV, the results from Sections 2.2 and 2.3 can be used. The gradient can be calculated by:

$$\left(\frac{\Delta OV}{\Delta T}\right) = \frac{(\frac{\Delta Gain}{\Delta T})}{(\frac{\Delta Gain}{\Delta OV})} \tag{5}$$

With this, we get for the two SiPM types:

$$\left(\frac{\Delta OV}{\Delta T}\right)_{2mm^2} \approx (33 \pm 2)\frac{mV}{^{\circ}C} \tag{6}$$

$$\left(\frac{\Delta OV}{\Delta T}\right)_{4mm^2} \approx (31 \pm 1)\frac{mV}{^{\circ}C} \tag{7}$$

Therefore, the gradients for the two SiPM types agree to each other within the uncertainties. The reference gradient provided by the SiPM fabricant (HAMAMATSU) is 34 mV/ $^{\circ}C$. This is within the uncertainties for the $2mm^2$ SiPMs and deviates by 3σ for the $4mm^2$ SiPMs. The deviation from the value given by the manufacturers could be due to a temperature dependence of the other components on the tileboard including the preamplifier within the HGCROC.

3 Temperature Studies with Irradiated SiPMs

By the end of the lifetime of CMS, the expected dose for the hadronic calorimeter is expected to be $5 \cdot 10^{13} n/cm^2$ at $-30^{\circ}C$. At room temperature, the noise levels of such an irradiated SiPM should correspond to a SiPM irradiated up to $2 \cdot 10^{12} n/cm^2$. In order to test the behaviour of the tileboard by the end of lifetime in the experiment, two SiPM types (one with $2mm^2$ and one with $4mm^2$ area) were irradiated to this dose. With them, the goal was to study the temperature impact on the radiated SiPM's noise level.

3.1 Overvoltage correction

As the breakdown voltage decreases with lower temperature following the Equation 1, the supplied bias voltage should be adjusted with temperature in order to keep the OV constant. For this, the HGCROC provides a DAC parameter referred to as 'InputDAC', which can be used to change the bias voltage supplied to the SiPMs on the tileboard

within a certain range. However, the change of the InputDAC also affects the pedestal value of the pulses, which had to be corrected by a different HGCROC parameter. For this reason, the OV at a temperature T can be calculated using the OV dependence of temperature calculated in Section 2.4 and the gradient of the OV with the change in InputDAC:

$$OV(23°C) = OV(T) - \Delta T \cdot \left(\frac{\Delta OV}{\Delta T}\right) + \Delta InputDAC \cdot \left(\frac{\Delta OV}{\Delta InputDAC}\right) \quad (8)$$

In order to verify the functionality of this overvoltage correction method, SPS were taken at $0°C$ and $-13°C$ with corrected OV. Then, the corresponding gains were compared. From the results shown in Figure 9a, it can be seen that the percentage differences mostly stay within the final experiment's uncertainty of 10%. Therefore,the OV-correction method can be seen as successful. Furthermore, one can see a channel dependence of the percentage differences. From channel 47 to 50, as well as from channel 55 to 62, an increasing trend is visible. A possible reason for this could be a slight temperature gradient across the HGCROC during the measurements. However, this still has to be further investigated.

3.2 Noise Measurement

In order to investigate the noise behaviour of the irradiated SiPMs in terms of temperature, their pedestal peak was measured and fitted using a Gaussian. This was done for different temperatures from room temperature down to $-30°C$ at different OVs. The resulting RMS for 2 V is shown in Figure 9b for both SiPM types. Here, the measurements show that the noise reduces towards lower temperatures as expected. However, since many parameters within the tileboard, e.g the breakdown voltage, the leakage current and the dark count rate depend on the device's temperature, a proper fit function for the observed data was not found yet. Here, a further investigation on the noise behaviour has to be carried out.

4 Summary and Outlook

As a first measurement, the OV-dependence of the SiPM-gain was measured for all 16 channels from the tileboard prototype. For the analysis, a novel DNL correction was implemented in order to correct the DNL of the HGCROC which affects the data taken from the SiPMs. In the measurement, a systematically higher gain for the $2mm^2$ SiPMs than for the $4mm^2$ was observed. Using a linear fit, the gradient ($\frac{\Delta Gain}{\Delta OV}$) was found to be $(1.85 \pm 0.07)/V$ for the $2mm^2$ and $(1.31 \pm 0.13)/V$.
Afterwards, the tileboard was integrated into a climate chamber in order to test it at low temperatures. Here, the functionality of the board was verified down to a temperature of $-40°C$. Furthermore, ($\frac{\Delta Gain}{\Delta T}$) was determined from SPS-measurements at different temperatures from room temperature ($23°C$) down to $-30°C$. Here, a uniform slope of

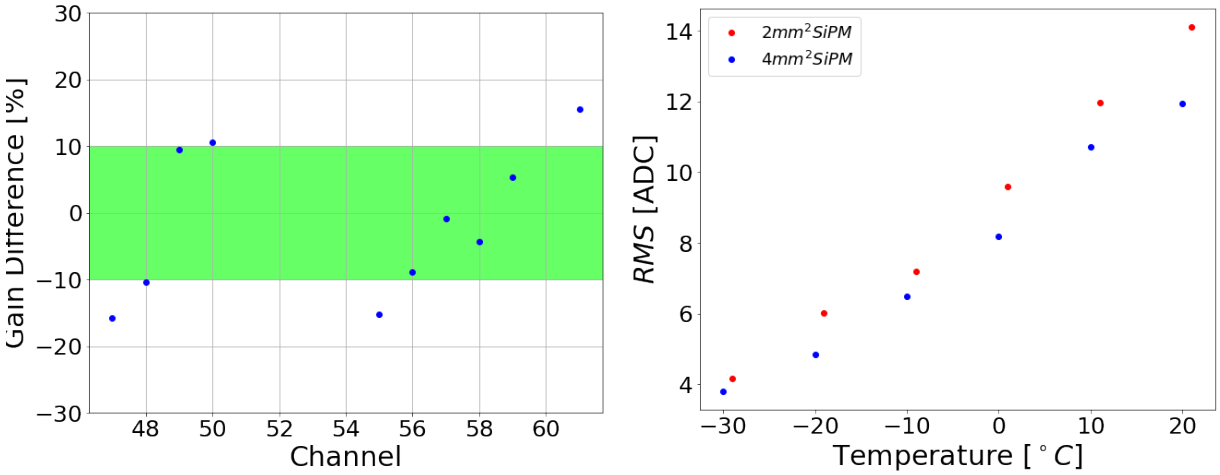

(a) Gain differences between measurements at $0°C$ and $-13°C$ in percent

(b) Noise Measurement at OV=2 V

Figure 9: Noise measurement using OV-correction method

in average $-0.05/°C$ was observed for both SiPM types.
From the two determined gradients, the OV dependence of the temperature ($\frac{\Delta OV}{\Delta T}$) was measured to be $(33 \pm 2)\frac{mV}{°C}$ and $(31 \pm 1)\frac{mV}{°C}$ for the $2mm^2$ and the $4mm^2$ SiPMs respectively. The difference in measured gradients to the gradients quoted by the manufactures could be due to the temperature affecting the electronics on the tileboard which requires further investigation. Additionally, the noise behaviour of two SiPMs, which were irradiated to the expected end-of-life dose at the CMS end caps at room temperature was investigated. For this, the change of the pedestal peak's RMS was measured for temperatures down to $-30°C$. As expected, the noise level reduced with lower temperatures. However, the exact noise function depends on various temperature dependent parameters and was not resolved within this project. Here, further investigations are needed to gain a better understanding of the device's noise behaviour.

References

[1] Mathias Reinecke. *The CMS High Granularity Calorimeter Scintillator/SiPM Tileboards*. TIPP Conference. 2021.

[2] Malinda de Silva. *Beam Tests of the First CMS HGCAL Tileboard Prototypes*. DPG Talk. 2020.

[3] Hermann Kolanoski. *Particle detectors : fundamentals and applications*. 2015.